

## THE VULTURE SURVEY: ANALYZING THE EVOLUTION OF Mg II ABSORBERS

NIGEL L. MATHES<sup>1</sup>, CHRISTOPHER W. CHURCHILL<sup>1</sup>, AND MICHAEL T. MURPHY<sup>2</sup>

*Draft version October 11, 2016*

### ABSTRACT

We present detailed measurements of the redshift path density, equivalent width distribution, column density distribution, and redshift evolution of Mg II absorbers as measured in archival VLT/UVES and Keck/HIRES spectra. This survey examines 432 VLT/UVES spectra from the UVES SQUAD collaboration and 170 Keck/HIRES spectra from the KODIAQ group, allowing for detections of intervening Mg II absorbers spanning redshifts  $0.1 < z < 2.6$ . We employ an accurate, automated approach to line detection which consistently detects absorption lines with rest-frame equivalent widths  $W_r \geq 0.02 \text{ \AA}$  in spectra with signal-to-noise greater than 40. We measure the equivalent widths, apparent optical depth column densities, and velocity widths for each absorbing system. Using our complete sample of all detectable Mg II absorbers, we can accurately determine the redshift path density of absorbers across cosmic time. We measure evolution in the comoving Mg II line density,  $dN/dX$ , finding more high equivalent width absorbers at  $z = 2$  than at present. We also measure evolution in the equivalent width and column density distributions, parameterized by a Schechter Function fit, finding a shallower weak-end slope at  $z = 2$ , owing to a relative increase in the number of strong Mg II absorbers at  $z = 2$ . Finally, we find little evolution in the cosmic mass density of Mg II absorbing systems from  $z = 0.1$  to  $z = 2.5$ . The relative increase in weak Mg II absorbers at low redshift likely stems from the weakening ionizing background in conjunction with the global rise in cosmic metallicity. The prevalence of strong Mg II absorbers near  $z = 2$  likely results from the increase in cosmic star formation, with Type II supernova creating and transporting more metal absorbing gas into the halos of galaxies at this time.

*per what?*

*Ambiguous/not clear.  
What does "increase  
at  $z = 2$ " mean?*

*This is quite  
long. Do you  
need all of it?*

*Keywords: galaxies: halos — quasars: absorption lines*

### 1. INTRODUCTION

One of the most important questions in modern studies of galactic evolution asks, how do baryons cycle into and out of galaxies, and how does this cycle determine the growth and evolution of galaxies themselves? More specifically, how does the process of gas accretion, star formation, and subsequent supernovae-driven feedback shape both the galaxy itself and the circumgalactic medium (CGM) surrounding the galaxy? By using spectroscopic observations of quasars, we can identify and analyze metal line absorbers in and around the halos of foreground galaxies. Though absorption line studies by themselves cannot directly answer these questions, the statistical results from such studies can provide vital information from which further progress can be obtained.

Perhaps one of the most prolific absorption features, the Mg II  $\lambda\lambda 2796, 2803$  doublet, traces cool ( $T \simeq 10^4 \text{ K}$ ; Churchill et al. (2003)) metal enriched gas in the disks and halos of galaxies. It is one of the best tracers of this gas because it can exist in a wide range of ionizing conditions, ranging in ionization parameter from  $-5 < \log U < 1$  (Churchill et al. 1999), it is observable in optical wavelengths from redshift  $0.1 < z < 2.6$ , and it has predictable line characteristics defined by its resonant doublet nature which make it ideal for automated searches.

The origin of Mg II absorbing gas is still debated. As summarized in Kacprzak et al. (2011) or Matejek et al. (2013), two separate interpretations exist to explain the origin of strong ( $W_r^{2796} > 0.3 \text{ \AA}$ ) and weak ( $W_r^{2796} < 0.3 \text{ \AA}$ ) Mg II absorbers. For the strong, higher equivalent width systems, multiple correlations exist between the rest frame Mg II equivalent width around galaxies and the host galaxy's star formation prop-

erties. Zibetti et al. (2007), Lundgren et al. (2009), Noterdaeme et al. (2010), Bordoloi et al. (2011), and Nestor et al. (2011) all found a correlation between  $W_r^{2796}$  and blue host galaxy color, showing that galaxies with more active star formation have more metal enriched gas in their halos. Bordoloi et al. (2014) also find that Mg II equivalent width increases with increasing star formation rate density. In addition, down-the-barrel spectroscopic observations of star forming galaxies often reveal strong Mg II absorption blueshifted  $300-1000 \text{ km s}^{-1}$  relative to the galaxy (Tremonti et al. 2007; Weiner et al. 2009; Martin & Bouché 2009; Rubin et al. 2010).

For the weak, lower equivalent width systems, it seems none of the above correlations hold. Chen et al. (2010), Kacprzak et al. (2011), and Lovegrove & Simcoe (2011) found little evidence for a correlation between galaxy color and Mg II equivalent width when restricting their samples to weak absorbers. Kacprzak et al. (2011) measured the orientation of galaxies relative to Mg II detections in the sight lines of background quasars and identifies co-planar gas around some galaxies, implying structures associated with accreting streams or filaments as opposed to outflows, which are more often observed perpendicular to the galaxy disk (Bordoloi et al. 2011; Kacprzak et al. 2012). Finally, the simulations of Stewart et al. (2011) and Ford et al. (2013) revealed a large reservoir of low-ionization, metal enriched, co-rotating gas around massive galaxies. Together, these studies paint a picture of the circumgalactic medium, as traced by Mg II, containing lower equivalent width systems tracing infalling gas and higher equivalent width systems tracing star formation driven outflows.

Nielsen et al. (2013b), using a sample of Mg II absorbers and their associated galaxies, examines both strong and weak Mg II absorbers from  $0.07 \leq z \leq 1.1$ . In Nielsen et al. (2013a), the authors find a more extended Mg II absorbing

<sup>1</sup> New Mexico State University, Las Cruces, NM 88003

<sup>2</sup> Swinburne University of Technology, Victoria 3122, Australia

*Centre for Astrophysics and  
Supercomputing, Swinburne ...*

*At this point, the introduction seems very unfocused. It's not really clear what problems will be addressed. I recommend a paragraph or few sentences, that summarizes the "discontinuities" in previous studies that this paper addresses.*

*Contradictory*

CGM around higher luminosity, bluer, higher redshift galaxies. In addition, in Nielsen et al. (2016), they find that bluer galaxies replenish their Mg II absorbing CGM through outflows, whereas red galaxies do not. Finally, in Nielsen et al. (2015), it is made clear that the largest velocity dispersions Mg II absorbing systems are measured around blue, face-on galaxies probed along their minor axis, strongly suggesting that these Mg II absorbers originate in bi-conical outflows.

Many surveys have been undertaken to inventory the cosmic nature and evolution of Mg II absorbers. The earliest studies (Lanzetta et al. 1987; Tytler et al. 1987; Sargent et al. 1988; Steidel & Sargent 1992) found that Mg II systems with rest equivalent widths above 0.3 Å show no evolution in  $dN/dz$  between redshifts  $0.2 < z < 2.15$ , with  $dN/dz$  increasing with redshift. These studies also found that the equivalent width distribution function,  $f(W_r^{\lambda 2796})$ , could be fit equally well with either an exponential or a power law function, leaving to question whether the cosmic distribution of Mg II in galactic halos exhibited a fractal, self-similar nature, or if there is a physical limit to size scale and quantity of Mg II absorbing gas.

Mg II absorption surveys have taken one of two different approaches to try to analyze the global distribution of Mg II absorbing gas across cosmic time. Churchill et al. (1999) and Narayanan et al. (2007) aimed to analyze the behavior of weak ( $W_r^{\lambda 2796} < 0.3 \text{ \AA}$ ) Mg II absorbers. They found that  $dN/dz$  increases from  $0 < z < 1.4$ , but then decreases for  $z > 1.4$ . In addition, they found the equivalent width distribution function for weak absorbers is best fit by a power law, strongly disfavoring an exponential fit to the overall distribution. These observations imply that from  $z \sim 2$  to present, weak Mg II absorbers become more prevalent, and these weak systems may exhibit self-similar behavior based upon the nature of power law distributions.

The most recent studies employ new multi-object spectrographs such as the Sloan Digital Sky Survey (SDSS) and the FIRE spectrograph on the Magellan Baade Telescope (Nestor et al. 2005; Matejek & Simcoe 2012). Nestor et al. (2005), examining over 1300 intervening Mg II absorbers in SDSS quasar spectra with  $W_r^{\lambda 2796} > 0.3 \text{ \AA}$ , found that the equivalent width distribution function is well fit by an exponential. They did not find evidence for redshift evolution in systems with  $0.4 < W_r^{\lambda 2796} < 2 \text{ \AA}$ , but saw fewer absorbers per comoving redshift path length with  $W_r^{\lambda 2796} > 2 \text{ \AA}$  as redshift decreases from  $z = 2$  to present. Matejek & Simcoe (2012), looking at 111 Mg II absorbing systems from  $1.9 < z < 6.3$  in infrared FIRE spectra, also found that the equivalent width distribution function is well fit by an exponential. They did note, however, that  $f(W_r^{\lambda 2796})$  steepens at redshifts below  $z = 3$ , showing again that the universal properties of Mg II absorbers seem to change approaching  $z = 2$ . They also observed that systems with  $W_r^{\lambda 2796} < 1.0 \text{ \AA}$  show no evolution with redshift, but stronger systems increase nearly three-fold in  $dN/dz$  from low redshift to  $z = 3$ .

Collectively, these surveys imply physical changes in the astrophysical processes or in the state of the gas structures in the environments giving rise to Mg II absorption as the universe ages. The properties of a given Mg II absorbing cloud are governed by the total amount of gas present, the gas phase metallicity, and the nature of the background radiation incident on the cloud.

As shown by Quiret et al. (2016), studying a large sample of Damped Ly $\alpha$  Absorbers (DLA's; neutral hydrogen ab-

sorbers with  $\log(N(\text{HI})) > 20.3$ ) and sub-DLA's ( $19.0 \text{ cm}^{-2} < \log(N(\text{HI})) < 20.3 \text{ cm}^{-2}$ ), the average metallicity of the circumgalactic medium increases from  $z = 5$  to  $z = 0$ . In addition, Ménard & Chelouche (2009) show that a correlation exists between the neutral hydrogen column density of an absorber and the rest frame Mg II equivalent width, with stronger Mg II absorbing systems having larger  $N(\text{HI})$ . As Mg II absorbers are often found associated with nearby galaxies, one can infer that the metallicity evolution of DLA's and sub-DLA's reflects an overall circumgalactic metallicity evolution, increasing from past to present (Kulkarni & Fall 2002; Prochaska et al. 2003; Kulkarni et al. 2005, 2007).

The cosmic ionizing background also changes dramatically from  $z = 2.5$  to  $z = 0$ . Haardt & Madau (2012) showed that the slope and intensity of the diffuse UV/X-ray ionizing background decreases from high redshift to low redshift, with a softer, weaker ionizing background present at low redshift. Specifically, the comoving 1 Rydberg emissivity decreases from  $\sim 2 \times 10^{23} \text{ erg s}^{-1} \text{ Mpc}^{-3} \text{ Hz}^{-1}$  at  $z = 2.5$  to  $\sim 70 \times 10^{23} \text{ erg s}^{-1} \text{ Mpc}^{-3} \text{ Hz}^{-1}$  at  $z = 0$ . Mg II absorbers are subject primarily to this UV background, with very little contribution from stellar radiation from a nearby galaxy (Churchill et al. 1999; Charlton et al. 2000; Rigby et al. 2002).

Behroozi et al. (2013) showed that cosmic star formation peaks around  $z = 2$ . At this point in time, galaxies are on average forming stars at a rate ten times greater than at  $z = 0$ . In conjunction with the fact that galactic-scale outflows can be driven by star formation (Zhu et al. 2015), and these outflows can eject Mg II absorbing gas to large galactocentric radii (Sharma & Nath 2013; Kacprzak et al. 2012; Nestor et al. 2011), it follows that more metal enriched gas, traced by Mg II absorbers, is being driven out of galaxies at  $z = 2$ .

We now aim to better understand the complex relationship between absorbing gas in the CGM/IGM and the physical processes shaping galaxy formation as the universe ages. For our survey, we will analyze the largest, most comprehensive sample of high resolution, high signal-to-noise quasar spectra to uniformly observe both strong and weak Mg II absorbers. We hope to finally rectify the discontinuities in prior Mg II absorption line surveys by analyzing large numbers of both strong and weak absorbers. To do so, we will examine quasar spectra observed with either the VLT/UVEES (Dekker et al. 2000) or KECK/HIRES (Vogt et al. 1994) spectrographs. We aim to characterize the evolution in the number density of all Mg II absorbers from present to beyond the peak of the cosmic star formation rate. We interpret these results in the context of global evolution in metallicity around galaxies, the ionizing background, and cosmic star formation.

We begin by explaining the methods of acquiring and analyzing the quasar spectra in Section 2. In Section 3, we present the results showing the evolution of the Mg II equivalent width distribution,  $dN/dX$ , and the Mg II column density distribution across redshift. We also analyze the functional fit to both the equivalent width and column density distributions. In Section 4 we discuss the redshift evolution of all types of Mg II absorbers and derive the relative matter density contributed to the universe by Mg II,  $\Omega_{\text{Mg II}}$ . In Section 5 we summarize our results and look to future studies using this rich data set, including a companion analysis of intervening C IV absorbers and detailed kinematic analysis of intervening absorbing systems. For all calculations, we adopt the most recently published Planck cosmology, with  $H_0 = 67.74 \text{ km s}^{-1} \text{ Mpc}$ ,  $\Omega_M = 0.258$ , and  $\Omega_\Lambda = 0.742$ .

*This is a lot strange. Why do Mg II's need to be introduced to reach this conclusion.*

*What?!*

*use a different form - this one doesn't make sense.*

*And? How does this contribute to the paper's motivation?*

*???*

*Kick Me! (a person's name, not an acronym)*

*DLAs (no apostrophe)*

This isn't true. For UVES, the flux cut-off depends a lot on what setting was used. For HIRES, the coverage is hardly ever so low as 3000, unless HIRES is refining.

## SQUAO

per what?

### THE VULTURE SURVEY

## 2. DATA AND ANALYSIS

### 2.1. Quasar Spectra Sample

We have assembled a sample of 602 archival quasar spectra observed with the VLT/UVES and KECK/HIRES spectrographs. The data originate from two archival data mining efforts - the UVES Squad collaboration (432 spectra) led by Michael Murphy, and the KODIAQ Survey (170 spectra) led by John O'Meara (O'Meara et al. 2015). The spectra range in signal-to-noise from 4 to 288, with the mean  $S/N = 38$ . Quasar emission redshifts span  $0.014 < z < 5.292$  and wavelength coverage for each spectrum spans either 3000–6600 Å or 3000–10,000 Å, depending upon whether the red arm of the spectrograph was used. We detect over 1180 Mg II absorbing systems from  $0.14 < z < 2.63$  to a detection limit of  $W_r^{\lambda 2796} \approx 0.02$  Å.

At what completeness level?

It's only low-order in small sections; there's many such sections! Need to say this.

SQL

"(Murphy 2016)"  
- see recent papers in MNRAS  
by me for citation formal. Use the DOI.

(ignore my scribbles...)

"because we found"

These depend on slit width and are not the same for all spectra

Ca

?? Why? If it is really discontinuous, then so is the flux...

Vague, un clear. If I don't know for sure what you've done, then probably no one else reading this will

### 2.2. Data Reduction and Line Detection

The KODIAQ data sample is reduced and fully continuum fit, delivered as normalized spectra according to the prescriptions of O'Meara et al. (2015). The UVES Squad sample also comes reduced, but with an automatic, low order polynomial continuum fit applied. This fit can incorrectly estimate the continuum around narrow emission regions and broad absorption features. For the UVES data sample, we add a higher order continuum fit to difficult regions of the spectra. We use UVES\_popler, an ESO/VLT UVES post-pipeline echelle reduction program written by Michael T. Murphy (Copyright 2003–2015 Michael T. Murphy) to apply these fits, preserving continuity of the continuum with non-absorbing regions.

The next step involves detecting all Mg II absorption features. We first limit the search range to regions of the spectrum redward of the Ly $\alpha$  emission, as Ly $\alpha$  forest contamination would render automatic detection of weaker metal lines nearly impossible. We also do not search 5000 km s $^{-1}$  blueward of the quasar emission redshift in order to avoid absorbers associated with the quasar itself. Finally, we exclude regions of strong telluric absorption bands, specifically from 6277–6318 Å, 6868–6932 Å, 7594–7700 Å, and 9300–9630 Å, finding that the molecular line separations and ratios can lead to numerous false positives when searching for Mg II doublets.

To find all intervening Mg II  $\lambda\lambda 2796, 2803$  absorbers, we employ a technique outlined in Zhu & Ménard (2013), in which we perform a matched filter search for absorption candidates detected above a certain signal-to-noise (S/N) threshold. The filter is a top hat function centered at the wavelength of the desired redshifted absorption line. Its width is selected to match the resolution of the spectrograph used (VLT/UVES  $\simeq 40,000$ ; KECK/HIRES  $\simeq 45,000$ ), set as the FWHM of an unresolved Gaussian absorption feature. We convolve the filter with the normalized spectrum to generate a normalized power spectrum in redshift space, with absorption features having positive power.

Because the error spectrum in both instruments is complicated and often discontinuous, we cannot convolve the filter with the error spectrum to derive normalized noise estimates, as is often done in matched filter analysis. Instead, we examine the noise in the derived power spectrum. We sigma clip chunks of the power spectrum before calculating its standard deviation. We take the standard deviation as the normalized noise and use it to calculate the signal-to-noise of the absorption features in the power spectrum as the ratio of

But you don't say anything of this! For SQUAO, I think you can refer to "Murphy et al. (in prep.; see also King et al. 2012 and Murphy et al. 2016 for descriptions of the data reduction, processing and continuum fitting)".

the normalized power ( $S$ ) to the normalized noise ( $N$ ). A flagged absorption feature has  $S/N > 5$ . A confirmed doublet detection for Mg II  $\lambda\lambda 2796, 2803$  requires detection of  $S/N^{\lambda 2796} > 5$  and  $S/N^{\lambda 2803} > 3$ . In addition, in our automated routines we remove detections with non-physical doublet ratios in unsaturated regions; specifically, we exclude cases where  $W_r^{\lambda 2803} > W_r^{\lambda 2796}$ , or  $W_r^{\lambda 2803} < (0.3 \times W_r^{\lambda 2796})$ . We relax this constraint in saturated features.

All absorption features are visually verified upon completion of the detection algorithm. Multiple feature detections within  $\pm 500$  km s $^{-1}$  of each other are grouped together to generate absorption systems to be analyzed. Once absorption systems are identified, we calculate the optical depth-weighted median absorption redshift to define the center of the entire absorption system. The formal derivation of this redshift is described in the appendix of Churchill & Vogt (2001).

We also derive an equivalent width detection limit across the spectrum. To do so, we model Gaussian features across the spectrum and assume a full-width at half-max (FWHM) defined by the resolution of the instrument to represent unresolved lines. The height of the Gaussian is then calculated as the height at which the modelled line would be detected using our matched filtering technique with a  $S/N = 5$ . We then integrate to find the equivalent width, and take that value as the minimum detectable equivalent width at a given wavelength. The detection algorithm is therefore self-monitoring. This full equivalent width detection limit spectrum will allow us to accurately characterize the completeness of our sample, along with the full redshift path length searched.

### 2.3. Measuring Absorption Properties

For each absorption system, we automatically define the wavelength bounds of each absorbing region by finding where the flux recovers past the  $1\sigma$  error spectrum for three pixels on either side of the absorption trough. Within these regions we calculate equivalent widths ( $W_r$ ), velocity widths ( $\Delta v$ ), kinematic spreads ( $\omega_v$ ), apparent optical depth (AOD) column densities ( $\log(N)$ ), and absorption asymmetries. The functional forms of these parameters are detailed in the appendices of Churchill & Vogt (2001), equations A3–A7.

## 3. RESULTS

### 3.1. Sample Characterization

Figure 1 shows the relationships between the measured absorption parameters, characterizing the distribution of absorption properties for our survey. With redshift, there are no obvious trends other than the highest equivalent width absorbers, with  $W_r^{\lambda 2796} > 4$  Å, existing at  $z > 1.5$ . The data gaps at  $z = 1.7$  and  $z = 2.4$  represent the larger omitted search regions which overlap with the stronger telluric absorption bands. With column density, we see the normal trends of higher column density systems exhibiting higher equivalent widths and velocity spreads, with the distributions asymptoting near  $\log N \simeq 15$  cm $^{-2}$  due to saturation effects and the nature of measuring column densities with the AOD method. With respect to kinematic spread, we observe the saturation line in the  $\omega_v$  vs.  $W_r^{\lambda 2796}$  relationship, showing the maximum  $\omega_v$  for a flat-bottomed absorption profile of a given equivalent width.

### 3.2. Sample Completeness and Survey Path Coverage

Figure 2 shows the function  $g(W_r^{\lambda 2796}, z)$ . This heat map details the number of spectra in which a Mg II  $\lambda\lambda 2796, 2803$

Any consideration of the uncertainty on these quantities ??

do you mean that that is one absorber? Not clear.

mean or median? Why does weighting matter if it's a median? And what about saturated regions? They have undefined optical depth!

"maximum" and no hyphen also

rest-frame

Unclear

Is this really a "power spectrum"? I don't think so, but I could well be wrong. It's still a flux spectrum as far as I can tell.

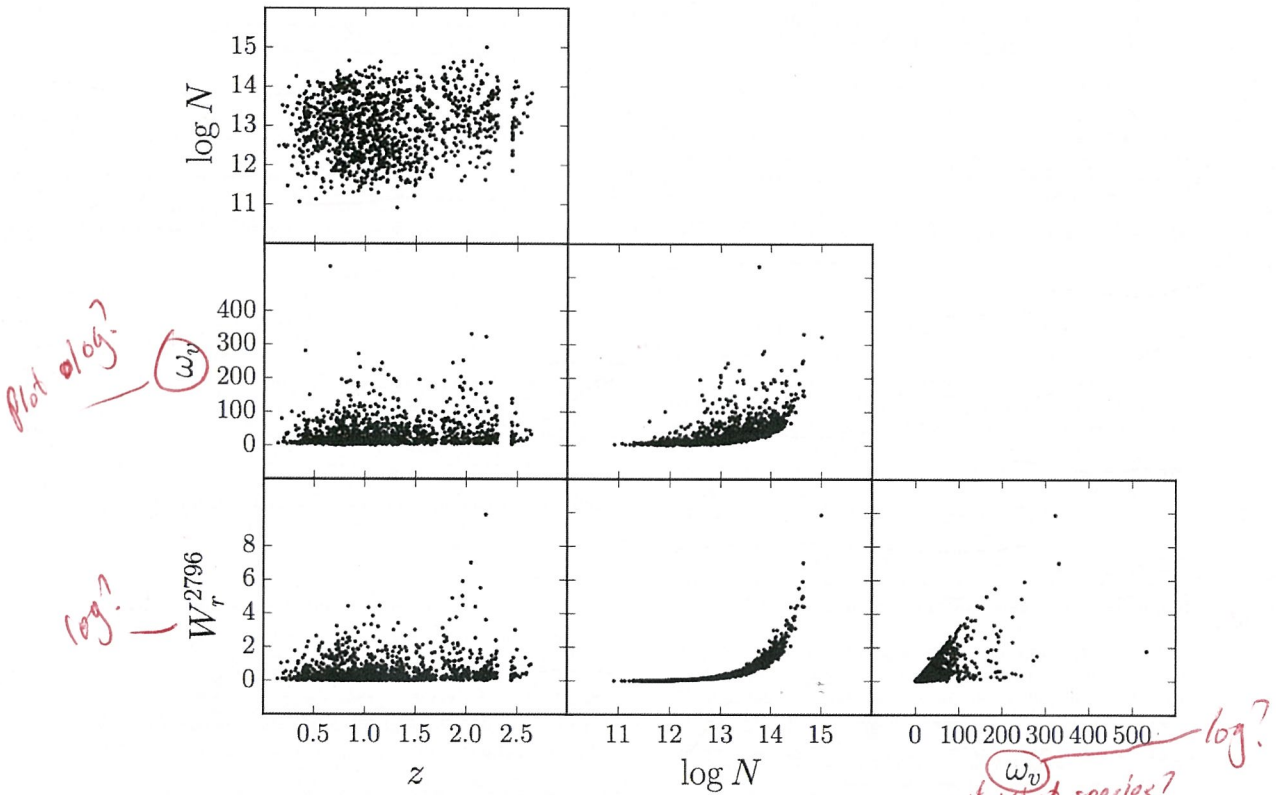


**Figure 1.** Correlations between measured absorption properties for survey sample.  $\log N$  is the AOD column density,  $\omega_v$  is the kinematic spread,  $W_r^{2796}$  is the rest frame Mg II $2796$  equivalent width, and  $z$  is the absorption redshift.

doublet could be detected as a function of the equivalent width detection limit and redshift. The vertical stripes with no redshift path coverage represent the omitted telluric absorption regions for our survey. The integral along a given  $W_r^{2796}$  slice gives the total redshift path length available for the sample ( $\Delta Z$ ).

### 3.3. $dN/dz$ and $dN/dx$

The largest sample of quasar spectra originates from the Sloan Digital Sky Survey (SDSS), with more than  $10^5$  spectra at present, which employs a spectrograph with an instrumental resolution around  $69 \text{ km s}^{-1}$ , limiting SDSS absorption surveys to strong absorbers (Nestor et al. 2005; Zhu & Ménard 2013). Conversely, previous studies of weak absorbers used small samples of quasar spectra, never exceeding 100 quasar spectra (Steidel & Sargent 1992; Narayanan et al. 2007; Kacprzak et al. 2011). In this paper, we aim to characterize the evolution of the incidence rate, number of absorbers per redshift path length, comoving line density, and cosmic mass density of all Mg II absorbers above a detection limit of  $W_r^{2796} > 0.01 \text{ \AA}$  from redshifts  $0.18 < z < 2.57$ .

You don't use a constant value throughout. Sometimes it's 0.018 and other times it's 0.028. What is it? Be consistent

The number of Mg II absorbers per redshift path length and its associated variance is defined as

$$\frac{dN}{dz} = \sum_i \frac{1}{\Delta Z_i(W_r)}, \quad \sigma_{\frac{dN}{dz}}^2 = \sum_i \left[ \frac{1}{\Delta Z_i(W_r)} \right]^2, \quad (1)$$

where we count the number of Mg II absorbers, dividing by the total searched redshift path length ( $\Delta Z$ ), defined as

$$\Delta Z_i(W_r) = \int_{z_1}^{z_2} g_i(W_r, z) dz, \quad (2)$$

where  $g_i(W_r, z)$  is the equivalent width sensitivity function at a given equivalent width detection limit. Equation (6) in Lanzetta et al. (1987) defines  $g(W_r, z)$ , which counts the number of spectra in which a given equivalent width absorption feature may be detected at the  $5\sigma$  level in a given redshift interval.

The comoving Mg II line density and its associated variance is defined as

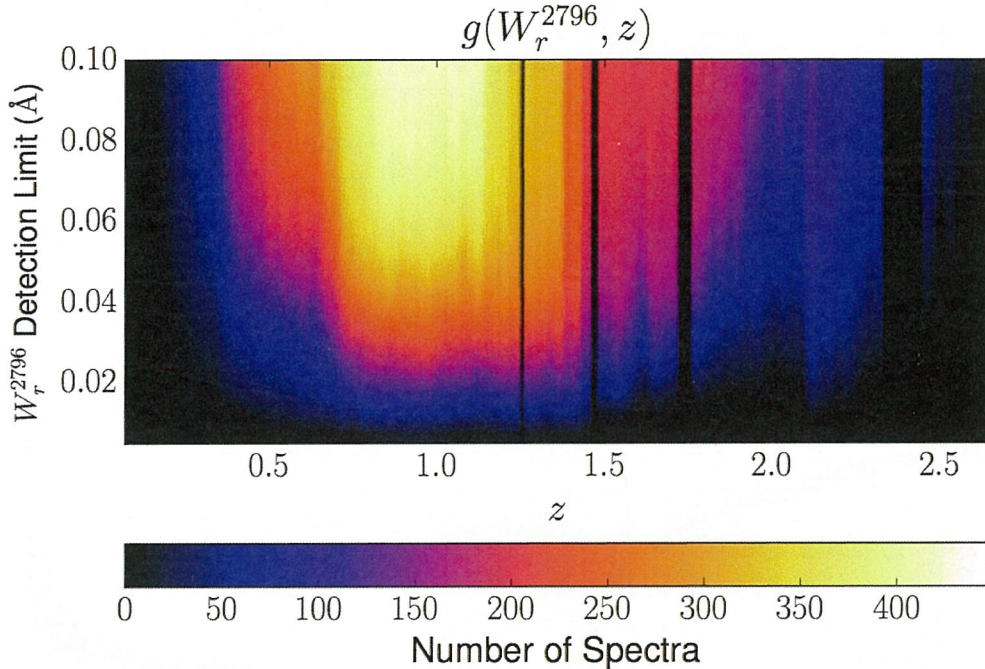


**Figure 2.** The function  $g(W_r^{2796}, z)$  shown as a heat map with the colors representing the value of  $g(W_r^{2796}, z)$ . This is the number of spectra in which an absorption line of a given equivalent width and a given redshift may be detected according to the detection limit of the spectrum. The vertical black bars representing no redshift path length coverage show the omitted wavelength regions of the survey based upon contaminating telluric absorption features.

$$\frac{dN}{dX} = \sum_i \frac{1}{\Delta X_i(W_r)}, \quad \sigma_{\frac{dN}{dz}}^2 = \sum_i \left[ \frac{1}{\Delta X_i(W_r)} \right]^2, \quad (3)$$

where we count the number of MgII absorbers, dividing by the total searched absorption path ( $\Delta X$ ), defined as

$$\Delta X_i(W_r) = \int_{z_1}^{z_2} g_i(W_r, z) \frac{(1+z)^2}{\sqrt{\Omega_M(1+z)^3 + \Omega_\Lambda}} dz, \quad (4)$$

where  $\Omega_M$  is the cosmic matter density, and  $\Omega_\Lambda$  is the cosmic density attributed to dark energy. Counting with respect to  $\Delta X$  accounts for both cosmological expansion along the line of sight and the transverse separation with objects with unchanging number density and cross section, allowing for more consistent comparisons across redshifts.

In Figures 3(a) and (b), we plot  $dN/dz$  and  $dN/dX$ , respectively, as a function of redshift for different minimum equivalent width thresholds, such that detected MgII absorbers have equivalent widths greater than  $W_{r,\min}^{2796}$ . Dotted lines are fit according to the analytical form which allows for redshift evolution in  $dN/dX$ , defined as,

$$f(z) \equiv n(z) \sigma(z) = n_0 \sigma_0 (1+z)^\epsilon, \quad (5)$$

where  $n_0$  is the comoving number density of MgII absorbers at  $z = 0$ ,  $\sigma_0$  is the absorbing cross-section at  $z = 0$ , and  $\epsilon$  is the evolution parameter, defined as the power dependence of  $dN/dX$  on redshift. We find that the best-fit value of  $\epsilon$  is negative when analyzing the full sample of MgII absorbers, including all detections with measured equivalent widths above  $W_r^{2796} > 0.01 \text{ \AA}$ .  $\epsilon$  then increases with subsequently larger minimum equivalent width thresholds, becoming positive for absorbers with  $W_{r,\min}^{2796}$ . This trend is driven primarily by an enhancement in  $dN/dX$  for the strongest MgII absorbers around  $z = 2$ , relative to lower redshifts. Conversely, at low redshift we observe more weak MgII absorbers. We show in Table 1 the values of the fit parameters for varying  $W_{r,\min}^{2796}$ , along with their errors.

In Figures 4(a) and (b), we show the values of  $n_0 \sigma_0$  and  $\epsilon$  as a function of  $W_{r,\min}^{2796}$ . The shaded red areas represent the  $1\sigma$  standard deviations derived from the fits to the  $dN/dX$  distribution. We show first that the co-moving density of absorbers multiplied by the absorber cross section for MgII decreases

But the graph doesn't show that

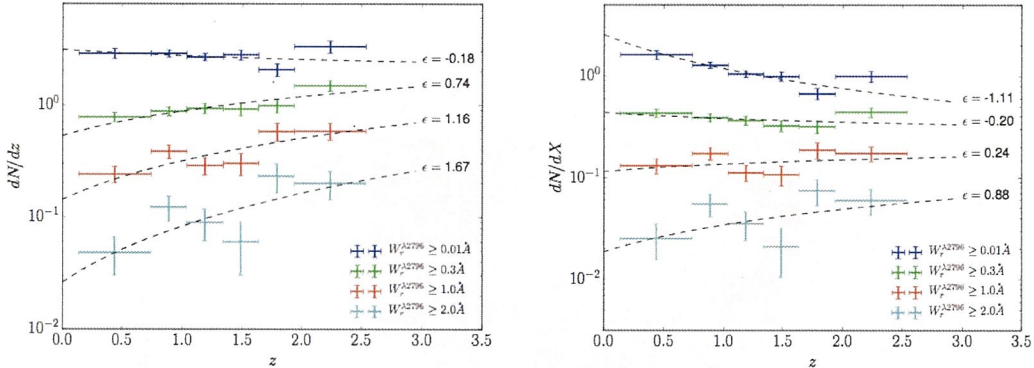
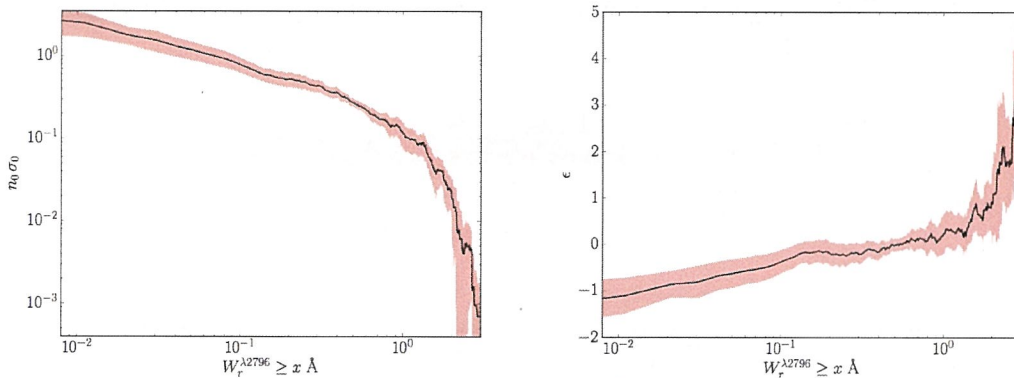


**Figure 3.**  $dN/dz$  and  $dN/dX$  as a function of redshift for different minimum equivalent width thresholds,  $W_r^{\lambda 2796}$ . Colors represent different  $W_r^{\lambda 2796}$ . The black dotted lines are fits to the distribution of the functional form  $f(z) = n_0 \sigma_0 (1+z)^\epsilon$ , with the best fit  $\epsilon$  value labelled. We see increasing values of  $\epsilon$  with increasing equivalent width, driven by an enhancement of stronger Mg II absorbers around redshift 2 compared to lower redshifts.



why can't one increase while the other decreases more strongly?

**Figure 4.** (a) The comoving number density of absorbers multiplied by the absorbing cross section, derived by fitting Equation 5 to  $dN/dX$ , as a function of  $W_r^{\lambda 2796}$ . As we examine samples with increasing minimum Mg II equivalent width thresholds, either the space density of absorbing cloud structures decreases, the absorbing cross-section decreases, or both parameters decrease. (b) The redshift evolution parameter,  $\epsilon$ , as a function of  $W_r^{\lambda 2796}$ . Weak Mg II absorbers are more abundant at low redshift, leading to a negative coefficient  $\epsilon$ . Absorbers with equivalent widths near 0.3 Å do not evolve, with  $\epsilon \simeq 0$ . Strong Mg II absorbers evolve away at low redshift, showing a large positive  $\epsilon$  increasing towards  $z = 2$ .

**Table 1**  
Parameterization of  $dN/dX$

$W_r^{\lambda 2796}$ [Å]	$n_0 \sigma_0$ [cm <sup>-1</sup> ]	$\epsilon$
0.01	$2.552 \pm 0.840$	$-1.11 \pm 0.39$
0.30	$0.438 \pm 0.077$	$-0.20 \pm 0.22$
1.00	$0.115 \pm 0.042$	$0.24 \pm 0.44$
0.01	$0.019 \pm 0.014$	$0.88 \pm 0.85$

as a function of  $W_r^{\lambda 2796}$ . This implies that there are fewer high equivalent width Mg II absorbers, and/or that they exist in smaller absorbing structures. We also show that the slope of the redshift dependence,  $\epsilon$ , increases as a function of  $W_r^{\lambda 2796}$ . This evolution parameter,  $\epsilon$ , changes from negative to posi-

tive toward higher equivalent width Mg II absorbers, implying that strong Mg II absorbers evolve away from  $z = 2$  to present, and that weak Mg II absorbers preferentially take their place. We observe minimal evolution with redshift in absorbers with equivalent widths between  $0.2 < W_r^{\lambda 2796} < 1$  Å.

#### 3.4. Equivalent Width Frequency Distribution

To calculate the equivalent width frequency distribution  $f(W)$ , the number of absorbers of a given equivalent width per unit path density, we calculate  $dN/dz$  or  $dN/dX$  for each equivalent width bin and divide by the bin width. We split the sample into four redshift regimes, ensuring that the number of absorbers in each redshift subsample remains constant. The result is a characteristic number of Mg II absorbers per redshift or absorption path length per equivalent width.

In Figures 5(a) and (b), we plot the equivalent width frequency distribution with respect to either  $dN/dz$  or  $dN/dX$ .

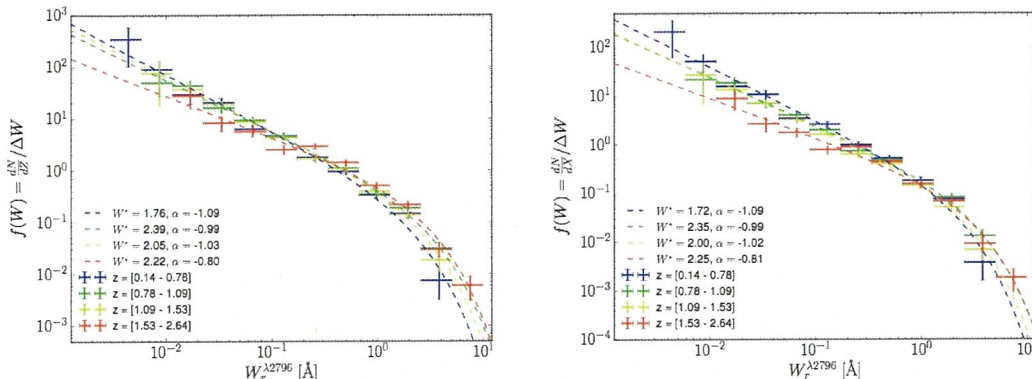


**Figure 5.** (a) The equivalent width distribution of Mg II absorbers, defined as the redshift path density ( $dN/dz$ ) in each equivalent width bin divided by the bin width. (b) The equivalent width distribution, defined as the comoving line density ( $dN/dX$ ) in each equivalent width bin divided by the bin width. We fit each distribution with a Schechter function, capturing the self-similar power law behavior of weak Mg II absorbers and the exponential power law cutoff when observing the strongest Mg II systems.

**Table 2**  
Schechter Fit to  $f(W) = \frac{dN}{dX}/\Delta W$

Redshift Range	$\Phi^*$ [ $\text{\AA}^{-1}$ ]	$W^*$ [ $\text{\AA}$ ]	$\alpha$
0.14–0.78	$0.24 \pm 0.09$	$1.72 \pm 0.68$	$-1.09 \pm 0.09$
0.78–1.09	$0.26 \pm 0.06$	$2.35 \pm 0.81$	$-0.99 \pm 0.06$
1.09–1.53	$0.21 \pm 0.03$	$2.00 \pm 0.35$	$-1.02 \pm 0.04$
1.53–2.64	$0.25 \pm 0.09$	$2.25 \pm 0.87$	$-0.81 \pm 0.12$

We fit each distribution with a Schechter function of the form,

$$\Phi(W_r) = \frac{\Phi^*}{W_r^*} \left( \frac{W_r}{W_r^*} \right)^\alpha e^{-W_r/W_r^*}, \quad (6)$$

where  $\Phi^*$  is the normalization,  $\alpha$  is the low equivalent width power-law slope, and  $W_r^*$  is the turnover point in the distribution where the low equivalent width power law slope transitions into an exponential cutoff. Table 2 shows the values of  $\Phi^*$ ,  $W_r^*$ , and  $\alpha$ , along with their associated errors. This functional fit is motivated by papers such as Kacprzak & Churchill (2011). The power law nature of the distribution of weak absorbers is apparent, and the exponential cutoff is motivated by physical limits to the size, density, and velocity widths of Mg II absorbing clouds. Examining the distribution as a function of redshift, we find the low equivalent width slope steepens from  $z = 2$  to present, with  $\alpha = -0.8$  in our subsample with  $1.53 < z \leq 2.64$  and  $\alpha = -1.07$  in our subsample with  $0.14 \leq z < 0.78$ . We observe a relative decrease in weak Mg II absorbers and a relative increase in strong Mg II absorbers from low redshift to redshifts near  $z = 2$ .

### 3.5. Column Density Distribution

To calculate the column density distribution, the number of absorbers of a given column density per unit path density, we calculate  $dN/dz$  or  $dN/dX$  for each column density bin and divide by the bin width. The result is a characteristic number density of Mg II absorbers per redshift or absorption path length as a function of their column densities. It should be noted that at high column densities near

**Table 3**  
Schechter Fit to  $f(N) = \frac{dN}{dX}/\Delta N$

Redshift Range	$\Phi^*$ [ $\text{cm}^2$ ]	$N^*$ [ $\times 10^{14} \text{ cm}^{-2}$ ]	$\alpha$
0.14–0.78	$0.15 \pm 0.06$	$1.70 \pm 0.96$	$-1.14 \pm 0.08$
0.78–1.09	$0.14 \pm 0.02$	$1.95 \pm 0.73$	$-1.09 \pm 0.03$
1.09–1.53	$0.10 \pm 0.02$	$2.67 \pm 0.98$	$-1.12 \pm 0.04$
1.53–2.64	$0.17 \pm 0.05$	$2.36 \pm 1.31$	$-0.91 \pm 0.08$

$\log(N(\text{Mg II})) = 15 \text{ cm}^{-2}$ , the measured column densities are lower limits as the AOD method to measure column densities cannot constrain the true column when the absorption line becomes saturated.

In Figures 6(a) and (b), we plot the column density frequency distribution using either  $dN/dz$  or  $dN/dX$ . Again, we fit this distribution with a Schechter function of the same form as Equation 6, except with equivalent width replaced with column density. Table 3 shows the values of  $\Phi^*$ ,  $N^*$ , and  $\alpha$ , along with their associated errors. We find again that the low column density end of the distribution becomes shallower as one goes from low redshift to  $z = 2$ . Due to saturation effects, the final high column density bin is best regarded as a lower limit.

## 4. DISCUSSION

We have shown a full cosmic inventory of Mg II absorbing gas from  $0.1 < z < 2.6$ , measuring  $dN/dz$ ,  $dN/dX$ , the equivalent width distribution, and the column density distribution down to detection limits as low as  $W_r^{\text{A2796}} = 0.02 \text{ \AA}$ .

Parameterizing  $dN/dX$  as a function of minimum equivalent width threshold, where we consider all absorbers with rest frame equivalent widths above a given  $W_{r,\min}^{\text{A2796}}$ , we find that the comoving opacity of Mg II absorbers,  $n_0 \sigma_0$ , decreases as equivalent width increases. We also find that the highest equivalent width systems evolve away from  $z = 2$  to present, while weaker, lower equivalent systems take their place.

The data also reveal that the equivalent width and column density distributions of Mg II absorbers are well represented by a Schechter Function. Examining the equivalent width dis-

but you include it in the fit? why?  
It will affect the  $N^*$  parameter a lot then?

Add sentences to spell out scope of this section

So? This just repeats the result from above but doesn't discuss if, which is what this section should do.

?? I don't know what you even mean by this!

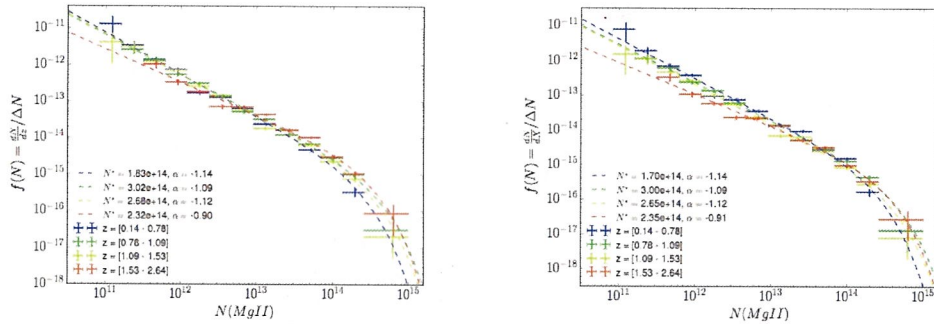


Figure 6. (a) The column density distribution of Mg II absorbers, defined as the redshift path density ( $dN/dz$ ) in each column density bin divided by the bin width. (b) The comoving line density ( $dN/dX$ ) in each column density bin divided by the bin width. We fit this distribution with a Schechter function to accurately parameterize the low column density power law slope and the exponential cutoff and high column densities.

Again, this just  
restated the  
result without  
discussion.

tribution for different redshift regimes, we find that at higher redshifts near  $z = 2$ , the low equivalent width slope flattens from  $\alpha = -1.09$  to  $\alpha = -0.81$ .

#### 4.1. Evolution of Mg II Distributions

Narayanan et al. (2007) measure the evolution of weak Mg II absorbers from  $0.4 < z < 2.4$  in VLT/UVES spectra. They compare to Churchill et al. (1999) which fits the equivalent width distribution with a power law, and to Nestor et al. (2005), which fits an exponential to  $f(W_r)$ . In the case of weak absorbers at  $z < 1.4$ , Narayanan et al. (2007) finds that a power law with a slope of  $\alpha = -1.04$  is a satisfactory fit, mirroring the results from Churchill et al. (1999). However, when examining the higher redshift half of their sample, they find a decreased number of weak Mg II absorbers and prefer the exponential fits of Nestor et al. (2005). Unfortunately, they do not also entertain the thought that a shallower power law slope, such as  $\alpha = -0.8$ , also accurately characterizes the equivalent width distribution of weak Mg II absorbers.

Narayanan et al. (2007) also analyze the evolution of  $dN/dz$  with redshift for weak Mg II absorbers. They find that the distribution follows the “no evolution” expectation; that is, the expected number density for a nonevolving population of absorbers in a  $\Lambda$ CDM universe, at redshifts less than  $z = 1.5$ . At higher redshift, they find that  $dN/dz$  for weak absorbers decreases. In Figure 7(a) we make a direct comparison with Narayanan et al. (2007), showing  $dN/dz$  for  $0.02 \leq W_r^{\lambda 2796} \leq 0.3 \text{ \AA}$  binned in the same manner as their Figure 4. Here, we observe that the relative peak in  $dN/dz$  for weak absorbers occurs near  $z = 0.75$ , as opposed to  $z = 1.2$  in Narayanan et al. (2007). However, the overall shape of  $dN/dz$  for this low equivalent width population remains in good agreement, with the redshift number density decreasing towards  $z = 2$ . In Figure 7(b), we show  $dN/dX$  for weak Mg II absorbers. Here, we clearly see that low equivalent width absorbers evolve away towards  $z = 2$ , as the “no evolution” assumption would be a perfectly flat distribution.

Steidel & Sargent (1992), and later Nestor et al. (2005), examine the redshift evolution of  $dN/dz$  for strong Mg II absorbers with  $W_r^{\lambda 2796} > 0.3 \text{ \AA}$ . They find that the number density of strong Mg II absorbers per redshift path length increases from  $z = 0$  to  $z = 2$ , however they cannot derive the slope of this trend to sufficient accuracy to distinguish between an evolving population or a non-evolving popula-

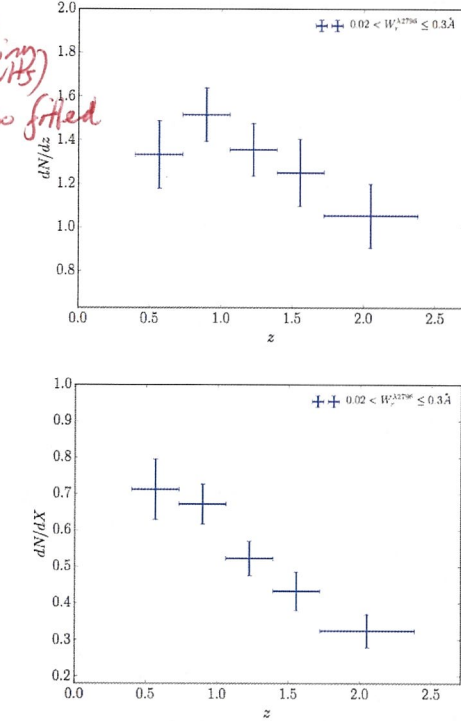


Figure 7. (a)  $dN/dz$  as a function of redshift for equivalent widths in the range  $0.02 < W_r^{\lambda 2796} \leq 0.3 \text{ \AA}$ . (b)  $dN/dX$  as a function of redshift for the same population. This equivalent width range comprises exclusively “weak” Mg II absorbers. These weak systems evolve away towards  $z = 2$ .

tion. We perform a similar analysis on our sample, calculating instead  $dN/dX$  to distill the analysis, as a flat distribution in  $dN/dX$  implies no evolution. When we take absorbers with  $W_r^{\lambda 2796} > 0.3 \text{ \AA}$ , we find that a fit to the function  $dN/dX = n_0 \sigma_0 (1+z)^\epsilon$  with a slope of  $\epsilon = -0.3$  is appropriate, implying that the comoving number density and/or cross-

What does that  
mean??

Ambiguous, from which  
direction? Use language this  
is clear and unambiguous.

Again, tense  
is confusing

You keep using this term but  
it could have many different  
meanings and I'm not sure  
which one you intend.

error bar

I really am confused about what you intend significantly here. Use much clearer language.

#### THE VULTURE SURVEY

9

section of strong Mg II absorbers does not evolve. However, when considering even stronger absorbers with  $W_r^{\lambda 2796} > 1 \text{ \AA}$ , we do observe evolution in  $dN/dX$ , with these strongest absorbers evolving away from  $z = 2$  to present. This evolution could be influenced by either an increase in the cosmic metallicity, a decrease in the ionizing background, or an increase in the total quantity of Mg II absorbing gas outside of galaxies. We suspect that the correlation between this enhancement and the cosmic SFR peak is not coincidence, and that these stronger Mg II absorption systems are direct byproducts of star formation driven winds in this same epoch.

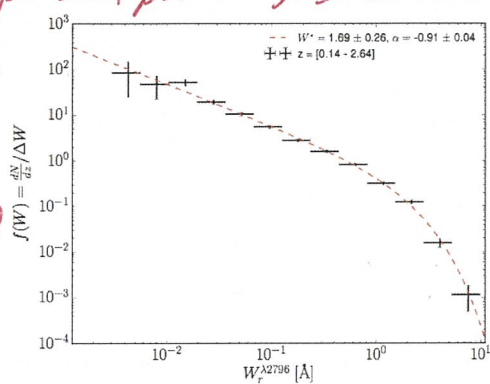


Figure 8. The equivalent width distribution of all detected Mg II absorbers, defined as the redshift path density ( $dN/dz$ ) in each equivalent width bin divided by the bin width. The cosmic distribution of absorbing Mg II is well fit by a Schechter function, with the parameters detailed in Equation 6.

*which sample? This is or the current one. These or those ("data" is plural.) uncertainty? sig figs.*

Kacprzak & Churchill (2011) combine multiple previous studies to characterize the equivalent width distribution function,  $f(W_r)$ . It is important to note, for comparison, that the sample with  $W < 0.3 \text{ \AA}$  spans redshifts from  $0.4 \leq z \leq 1.4$ , while the sample with  $W \geq 0.3 \text{ \AA}$  spans  $0.4 \leq z \leq 2.3$ . They find a Schechter function with a low equivalent width slope of  $\alpha = -0.642$  and an exponential cutoff of  $W^* = 0.97 \text{ \AA}$  best fit the data. In Figure 8, we perform the same analysis with the total sample of our survey, finding a faint end slope of  $\alpha = -0.9 \pm 0.04$  and an exponential cutoff at  $W^* = 1.69 \pm 0.26 \text{ \AA}$ . The primary point of contention here lies in the determination of  $\alpha$ , which is discrepant by more than  $3\sigma$  from the measurements of Kacprzak & Churchill (2011).

#### 4.2. $\Omega_{\text{MgII}}$

We now aim to calculate the matter density of Mg II absorbers across cosmic time. To do so, we employ the following equation,

$$\Omega_{\text{MgII}} = \frac{H_0 m_M}{c \rho_{c,0}} \int_{N_{\min}}^{N_{\max}} f(N_{\text{MgII}}) N_{\text{MgII}} dN_{\text{MgII}}, \quad (7)$$

where  $H_0$  is the Hubble constant today,  $m_M = 4.035 \times 10^{-23} \text{ g}$ ,  $c$  is the speed of light,  $\rho_{c,0}$  is the critical density at present,  $f(N_{\text{MgII}})$  is the column density distribution of Mg II absorbers, and  $N_{\text{MgII}}$  is the column density. Using our derived fit to the column density distribution, we are able to numerically inte-

grate the first moment from  $0 < N(\text{MgII}) < 20 \text{ cm}^{-2}$ . The results are shown below in Figure 9.

more labels.

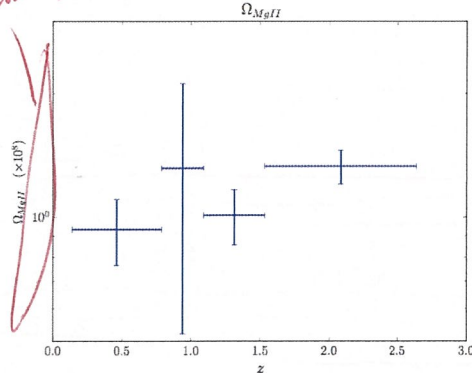


Figure 9.  $\Omega_{\text{MgII}}$  as a function of redshift. The cosmic mass density of Mg II stays roughly flat near a value of  $1 \times 10^{-8}$ , with a potential increase from  $z = 0.1$  to  $z = 2.5$ .

*to uncertainties with a bootstrap Monte-Carlo method truncated sentence?*

Errors are derived by bootstrap Monte-Carlo. We select random column densities, with replacement, from the sample of measured column densities for all of our Mg II absorbers until a sample size of 1180. We then recalculate the column density distribution, find the best parameterized Schechter fit, and then integrate and compute Equation 7. We perform this task 1024 times to develop a statistical distribution of values for  $\Omega$ . We take the standard deviation about the mean of this ensemble of simulated measurements as the error in  $\Omega_{\text{MgII}}$ . We find that the cosmic mass density of Mg II increases from  $z = 0$  to  $z = 2$ .

#### 4.3. Potential Causes for Trends

The most obvious conclusion to be drawn from our Mg II survey is that around redshift  $z = 2$ , physical changes occur in the distribution of Mg II absorbers. We find the following differences at  $z = 2$ :

1. The number of strong absorbers per unit path length increases.
2. The faint end slope of the equivalent width and column density distributions flattens.
3. The 'knee' of the Schechter fit of the equivalent width and column density distributions pushes outward to higher  $W_r^{\lambda 2796}$  and  $N(\text{MgII})$ .
4. The cosmic mass density of Mg II increases.

We can now confidently state that the physical properties driving the global distribution of Mg II absorbers changes around  $z = 2$ . Possible explanations relate to the ionization conditions in the halos of galaxies at this time, the metallicity of gas around galaxies, or the quantity of metals in the circumgalactic medium.

Haardt & Madau (2012) represents the most recent and robust estimate of the cosmic ionizing background as a function of redshift, which is the primary ionizing component responsible for the global ionization state of gas in galactic halos. From redshift  $z = 1.1$  to redshift  $z = 3.0$ , the comoving

Why does this stop here? The discussion should suggest a resolution to this. Also, we cannot tell that there's even a problem because you've not given the error bar on KAC II's value of  $\alpha$ . Also, aren't the  $W^*$  values also very different?

I don't think this is well-formed. The sample only goes up to  $z=2$ , so none of the plots go sufficiently higher than  $z=2$  to allow you to conclude that something happens "at"  $z=2$ . This either needs significant rewording, or the logic needs rethinking.

I'm very confused because of the use of "increasing", when neither time nor ~~actual~~ redshift is specified, and because you keep saying that quantity X "increases at  $z=2$ ", which doesn't make sense unless you say what it was "before" (and whether that relates to time,  $z$  or some other parameter).  
with time or  $z$ ?

emissivity increases dramatically for photon energies above 3 eV. As the number of ionizing photons in the IGM increases, holding constant the density and quantity of metals in galactic halos, we would nominally expect for the ionization parameter of absorbers in the halos of galaxies to increase. Increasing the ionization parameter alone should decrease the observed quantity of Mg II seen at  $z = 2$  relative to lower redshifts as Mg II favors lower ionization parameter conditions. This is not what we observe in our sample, and we therefore disfavor the hypothesis that changes in ionization conditions in the halos of galaxies could drive the observed increase in the number of strong Mg II absorbers at redshift  $z = 2$ .

The metallicity of galaxy halos as a whole is not well characterized over time. However, if we assume that the metals in galaxy halos are built up as a result of outflows (Quigley et al. 2016), and that the metallicity of the halo may scale with the metallicity of the ISM, then it would make no sense to observe larger quantities of Mg II in the circumgalactic medium at  $z = 2$  compared to  $z < 1$  because the metallicity should be higher at lower redshifts. In fact, under these assumptions, the metals should build up over time in the halos of galaxies, producing stronger Mg II absorption at lower redshift. Cosmic metallicity evolution alone, then, cannot drive the observed trends.

This leaves us, then, with the most likely conclusion being that galaxies eject more metals into their halos around  $z = 2$ . Behroozi et al. (2013) combines data from 19 independent studies from 2006–2012 of the cosmic star formation rate to find that it rises with significant scatter from  $z = 8$  to  $z = 2$ , where it peaks before falling off with a steeper slope towards  $z = 0$ . Galaxies at  $z = 2$  were forming stars at higher rates than any other time in cosmic history. In addition, studies associated with COS-Halos seeking to understand the distribution of metals around galaxies have found the majority of cool, metal absorbing gas lies within the virial radius of galaxies (Peeples et al. 2014). Stern et al. (2016) also find that the mean cool gas density profile around galaxies scales as  $R^{-1}$ , with most strong, low ionization metal absorbers existing near the galaxy itself.

Therefore, we now favor a picture where galaxies, undergoing their most vigorous stage of global star formation in cosmic history, expel large quantities of metal enriched gas into their halos through star formation driven outflows at  $z = 2$ .

## 5. CONCLUSIONS

Using archival data from VLT/UVES and KECK/HIRES, we have undertaken the most complete survey of Mg II absorbers in 602 quasar spectra in high resolution ( $\sim 7 \text{ km s}^{-1}$ ) for the detection of both strong and weak Mg II absorbers. Our survey spans absorption redshifts from  $0.18 < z < 2.57$ , allowing for characterization of the evolution of the distribution of these absorbers across cosmic time. Using our own detection and analysis software, we are able to accurately characterize the equivalent width detection limit, absorption path length, and survey completeness to a level allowing for an accurate determination of  $dN/dz$ , the equivalent width distribution function, the column density distribution function, and the total cosmic mass density of Mg II absorbers. Our main findings are as follows:

1. We find 1180 intervening Mg II absorption line systems with equivalent widths from  $0.003 \text{ \AA}$  to  $8.5 \text{ \AA}$ , and redshifts spanning  $0.14 \leq z \leq 2.63$ .

2. We present the distributions of the number of absorbers per unit redshift,  $dN/dz$ , and the comoving Mg II line density,  $dN/dX$ , as a function of minimum equivalent width threshold and as a function of redshift. We parameterize the evolution in  $dN/dX$  specifically with an empirical fit to the distribution in the form of  $dN/dX = n_0 \sigma_0 (1+z)^\epsilon$ , showing  $\epsilon$  increases from  $\epsilon = -1.11$  for all absorbers with  $W_r^{\lambda 2796} \geq 0.01 \text{ \AA}$  to  $\epsilon = 0.88$  for absorbers with  $W_r^{\lambda 2796} \geq 2 \text{ \AA}$ . Low equivalent width absorbers are more prevalent at low redshift, whereas the highest equivalent width absorbers are more prevalent near  $z = 2$ .

3. The equivalent width distribution function and the column density distribution function for Mg II absorbers are both well fit by a Schechter Function, with a characteristic normalization, faint end slope, and exponential cutoff. Both functions show redshift evolution, specifically in the faint end slope, with this slope becoming shallower for redshifts near  $z = 2$ . There exist proportionately more high equivalent width, high column density Mg II absorbers near  $z = 2$ .
4. The cosmic mass density of Mg II absorbing gas,  $\Omega_{\text{Mg II}}$ , increases from  $\Omega_{\text{Mg II}} \simeq 0.8 \times 10^{-8}$  at  $z = 0$  to  $\Omega_{\text{Mg II}} \simeq 1.3 \times 10^{-8}$  at  $z = 2.5$ .
5. We interpret these trends as owing to the increased star formation activity in galaxies at  $z = 2$ , ruling out other possible drivers such as changes in the ionizing radiation at these times and changes in the cosmic metallicity. This physical interpretation relies on galaxies creating more metal enriched gas at this time through supernovae driven winds, expelling it into the circumgalactic medium.

## Acknowledgements

## REFERENCES

- Behroozi, P. S., Wechsler, R. H., & Conroy, C. 2013, ApJ, 770, 57
- Bordoloi, R., Lilly, S. J., Kacprzak, G. G., & Churchill, C. W. 2014, ApJ, 784, 108
- Bordoloi, R., Lilly, S. J., Knobel, C., et al. 2011, ApJ, 743, 10
- Charlton, J. C., Mellon, R. R., Rigby, J. R., & Churchill, C. W. 2000, ApJ, 545, 635
- Chen, H.-W., Wild, V., Tinker, J. L., et al. 2010, ApJ, 724, L176
- Churchill, C. W., Rigby, J. R., Charlton, J. C., & Vogt, S. S. 1999, ApJS, 120, 51
- Churchill, C. W., & Vogt, S. S. 2001, AJ, 122, 679
- Churchill, C. W., Vogt, S. S., & Charlton, J. C. 2003, AJ, 125, 98
- Dekker, H., D'Odorico, S., Kaufer, A., Delabre, B., & Kotzlowski, H. 2000, in Proc. SPIE, Vol. 4008, Optical and IR Telescope Instrumentation and Detectors, ed. M. Iye & A. F. Moorwood, 534–545
- Ford, A. B., Oppenheimer, B. D., Davé, R., et al. 2013, MNRAS, 432, 89
- Haardt, F., & Madau, P. 2012, ApJ, 746, 125
- Kacprzak, G. G., & Churchill, C. W. 2011, ApJ, 743, L34
- Kacprzak, G. G., Churchill, C. W., Evans, J. L., Murphy, M. T., & Steidel, C. C. 2011, MNRAS, 416, 3118
- Kacprzak, G. G., Churchill, C. W., & Nielsen, N. M. 2012, ApJ, 760, L7
- Kulkarni, V. P., & Fall, S. M. 2002, ApJ, 580, 732
- Kulkarni, V. P., Fall, S. M., Lauroesch, J. T., et al. 2005, ApJ, 618, 68
- Kulkarni, V. P., Khare, P., Péroux, C., et al. 2007, ApJ, 661, 88
- Lanzetta, K. M., Turnshek, D. A., & Wolfe, A. M. 1987, ApJ, 322, 739
- Lovegrove, E., & Simcoe, R. A. 2011, ApJ, 740, 30
- Lundgren, B. F., Brunner, R. J., York, D. G., et al. 2009, ApJ, 698, 819
- Martin, C. L., & Bouché, N. 2009, ApJ, 703, 1394
- Matejek, M. S., & Simcoe, R. A. 2012, ApJ, 761, 112
- Matejek, M. S., Simcoe, R. A., Cooksey, K. L., & Seyffert, E. N. 2013, ApJ, 764, 9
- Ménard, B., & Chelouche, D. 2009, MNRAS, 393, 808
- Narayanan, A., Misawa, T., Charlton, J. C., & Kim, T.-S. 2007, ApJ, 660, 1093

Well, one could argue that ARA studies have done exactly that!

The galaxy's ISM

Is that true?? What if outflows are just more prominent at  $z < 2$  ???

But the previous paragraph assumed that "halos are built up as a result of outflows" ... I'm confused!

I don't follow the logic here. It needs to be more clearly explained or reworded/revised.